

MORPHOLOGICAL FEATURES OF LYMPHATIC AND MESOTHELIAL COMMUNICATIONS IN THE BROAD LIGAMENT OF THE PIG

T. Doboszynska, A. Andronowska, L. Janiszewska, A. Sobotka

Department of Reproductive Histophysiology, Division of Reproductive Endocrinology and Pathophysiology, Institute of Animal Reproduction and Food Research of Polish Academy of Sciences, Olsztyn, Poland

ABSTRACT

The broad ligament containing uterine, paraovarian, and oviduct lymphatics was examined in the pig in various phases of the estrous cycle using light, scanning and transmission electron microscopy. The architecture of these regions differed and was independent of the lymphangions of the precollector and collector lymphatic vessels. Lymphangions were separated from mesothelium by connective tissue and/or muscle layers; however, in the vicinity of the thin walled paraovarian sac, large lymphangions were often compressed between two epithelial layers. Numerous lymphatic lacunae were in direct contact with the peritoneal and paraovarian sac cavities. The mesothelial lining of the broad ligament and the external and internal epithelium of the pig paraovarian sac displayed two distinct cell types. Only smaller cuboidal cells with prominent microvilli extended above the lymphatic endothelium. The surfaces of these cells were discontinuous and showed: 1) lymphatic stomata, 2) small pores or fenestrae, 3) a superficial network of epithelial-free communications with underlying connective tissue to the paraovarian sac in the postovulatory period independent of the lymphatic vasculature, and 4) endothelial (instead of epithelial) cells with crevice-like

discontinuities in large portions of the internal sac surface during the follicular phase of estrus. Numerous lymphatic stomata had orifices composed of flattened cuboidal cells while lymphatic endothelial cells were characterized by macula or zonula adherent connections formed within rims of various sizes (up to 50 μm in diameter). During estrus, there were circular (0.5-2.0 μm) and irregular (to 10 μm) interendothelial openings in stomatal orifices with migrating cells.

These morphologic findings suggest that absorption and passage of fluid, particles and cells between cavities and the lymphatic lumen in areas of the paraovarian lymphatic plexus in the pig is feasible.

Our earlier studies demonstrated that lymphatics emanate from the ovary in the pig and parallel the mesovarium pedicle containing the blood vascular plexus (1). Most lymphatic precollectors of the uterine horn form ventral and dorsal superficial networks in the mesometrium that extend to the ovary. The precollectors join and become lymphatic collectors which, similar to those of the ovary, connect with regional lymph nodes (2), although there are no direct inter-lymphatic communications (3). Doboszynska et al (4) first demonstrated that in the subovarian area there was a characteristic

lymphatic plexus with tightly packed giant oval lymphangions (segments) that formed a special "mattress-like" infrastructure for the ovary. Gawronska et al (2) described lymphatic precollectors posteriorly exiting the uterine wall in the region bordering the oviductal isthmus. The lymph collectors leaving this plexus drained to the pelvic lymph nodes. The ultrastructural changes in mesometrial lymphatics (5,6) observed in estrous cycling pigs, raised the possibility that epithelial cavities connected with adjacent lymphatics.

The organization of mesothelial cells lining the peritoneal surface has been studied to determine their connections with lymphatics and thereby the potential pathway(s) of peritoneal fluid and particulate absorption in several species. Stomata, fenestrae, gaps, pores both in the mesothelial and submesothelial lacunae (review 7), and macula cribiformis (8-11) were considered to play an important role and fluid absorption including that of the diaphragm. Despite these observations, fluid in particulate absorption in the broad ligament has received less attention. One exception has been the ovarian bursa in the golden hamster which encircles the ovary as a closed bag with contained fluid (12,13). Sinohara et al (14) demonstrated that stomata connect the bursal cavity with the lumen of the lymphatics and are consistently present throughout estrus; however, these lacunae vary in response to changes in the bursal cavity during the estrous cycle. Crevice-like gaps with the subepithelial connective tissue exposed to the bursal cavity and smooth-surfaced areas lined with lymphatic endothelium instead of bursal epithelium have also been described (15).

The purpose of the present study was to examine using light, scanning and transmission electron microscopy whether in the porcine mesothelium and submesothelial tissues of the broad ligament and paraovarian sac there is morphologic evidence that favors fluid and particulate absorption directly into lymphatic vessels of the paraovarian plexus.

MATERIALS AND METHODS

Twelve sexually mature pigs in paraovular (n=3), luteal (n=5) and follicular phases (n=4) of the estrous cycle (day 0 detected with vasectomized boar) of similar age (10-12 months) were studied. Anesthetized pigs were laparotomized, and the reproductive organs with the broad ligament were removed. The right-sided portion of the broad ligament was excised and fixed with a solution of 2.5% glutaraldehyde and 2% paraformaldehyde in 0.1 M cacodylate buffer, pH 7.4 (Karnovsky fixative) by immersion (4 h). The contralateral left-sided portion of the broad ligament was taken for light microscopy and processed as outlined below.

Light Microscopy (LM)

Fragments of "left-ligaments" (10/10 mm) from the mesometrium near the paraoviductal region of the uterine horn, and mesosalpinx adherent to the isthmus (preplexus lymphatics), paraovarian sac subampullary and subinfundibular areas, mesometrium from para-subovarial areas containing the lymphangions of the paraovarian lymphatic plexus and draining lymphatic collectors (postplexus lymphatics) were stained with a silver technique to darken the epithelial and endothelial cell boundaries (16). The adjacent tissues were fixed with Bouin's solution for serial sections stained with hematoxylin and eosin (H&E) to determine the relationship of the lymphatics with mesothelium and peritoneum. Additionally, these lymphatics were filled with carmin-gelatin and India ink by injections into the subserosal connective tissue (2), and serial cross-sections taken for light microscopy.

Scanning Electron Microscopy (SEM)

After initially fixing the "right-ligament" tissues with intact mesothelium or exposed submesothelium, connective tissue (10-20

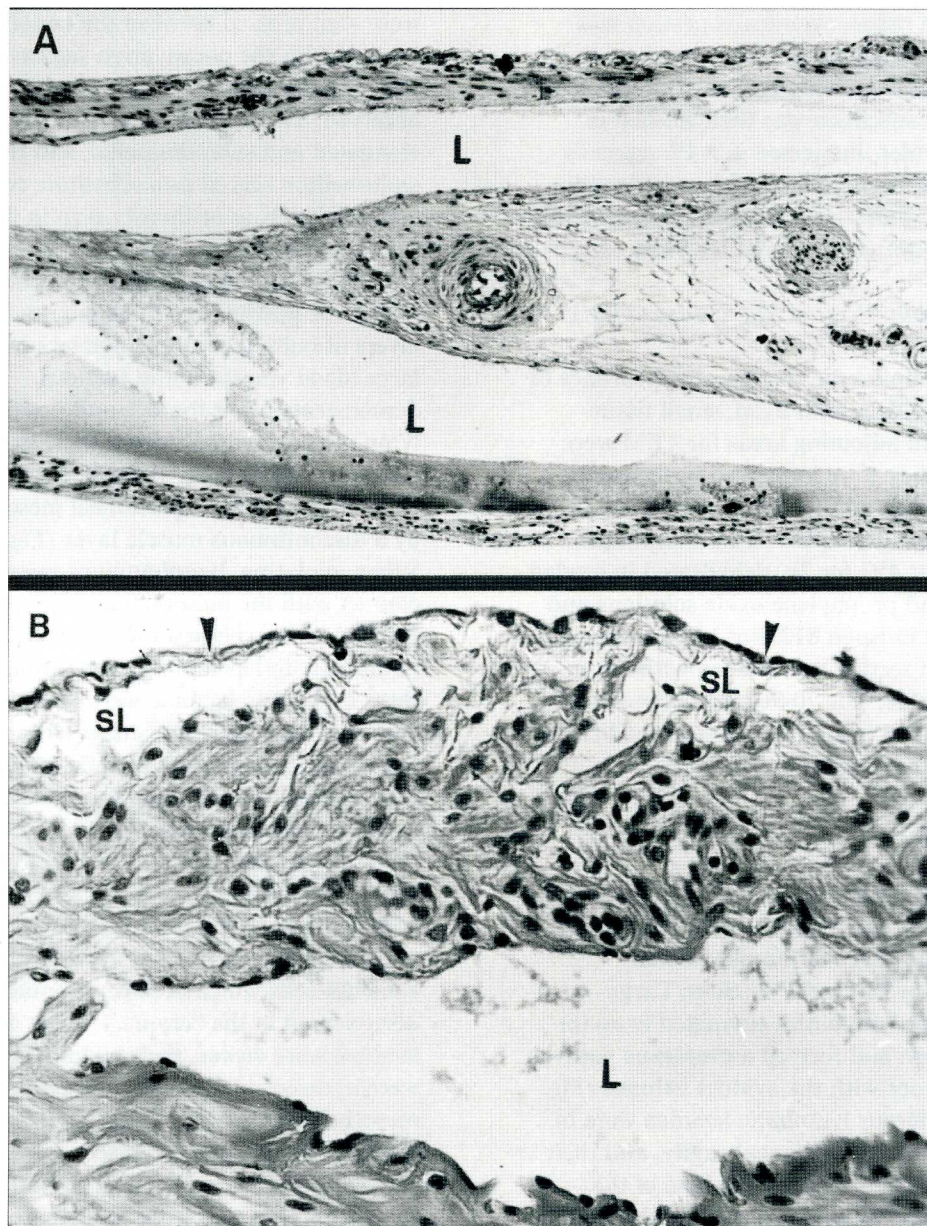


Fig. 1. Fragments of the suboviductal isthmus mesentery with large precollector lymphangions (L) of preplexus uterine pathways in the luteal phase of the estrous cycle. These lymphangions are separated by submesothelial loose connective tissue (A, x50) in which lymphatic lacunae (SL) are seen directly beneath a discontinuous mesothelium (arrowheads) (B, x500). H&E.

mm²) was taken from areas as previously described. Fragments of the uterus and oviduct with intact visceral peritoneum were also excised for comparison.

Tissues were sectioned into four samples and mounted on a cork with two mesothelial surfaces and postfixed in Karnovsky fixative at 4 °C for 2 h. To expose the submesothelial

connective tissue, chemical digestion was carried out with 2N NaOH at room temperature for 4-6 days to digest cellular elements (17). Each specimen was then washed in distilled water, immersed in a 1% aqueous solution of tannic acid for 2 h, postfixed in cacodylate-buffered 1% osmium tetroxide for 2 h and routinely prepared for SEM.

Transmission Electron Microscopy (TEM)

To compare the structural appearance of stomatal orifices with SEM, small tissue blocks from adjoining areas for TEM were excised. They were immersed in the same fixative for an additional 2h, post-fixed in cacodylate buffer (pH=7.4), 2% osmium tetroxide at 4°C for 2h, dehydrated in graded ethanol and propylene oxide solutions and embedded in Epon 812. For LM-viewing, a 0.5-1.0 µm section was stained with 1% toluidine blue. The 70-90 nm sections were stained with a uranyl acetate and lead citrate and examined by TEM.

RESULTS

The general architecture of the peritoneal side of the broad ligament with lymphatics forming the paraovarian plexus was examined by LM serial sections. Large precollector lymphatics emanated from the uterine horn and formed a preplexus pathway on the border with the oviduct isthmus (*Fig. 1A*). Numerous lymphatic lacunae were in contact with the peritoneal cavity, and their endothelial cells reached the base of the mesothelium without intervening tissue (*Fig. 1B*). The lymphatic stomata were open and in the follicular phase of the estrous cycle were particularly numerous (see below). In localized thick walls of membranes, suspended oviductal ampulla and infundibulum (paraovarian sac walls), large lymphangions surrounded blood vessels near the epithelial layer, and the lymphatic endothelium was separated by connective tissue (*Fig. 2A*). In the region of thin walls, large lymphatics

were seen pressed between the endothelium in contact with the paraovarian sac cavity (*Fig. 2B*). Typical lymphatic lacunae were also observed. The lacunae were commonly elongated and submesothelial, and the thin endothelium served as a substitute cover for epithelial cells as ordinarily seen in the pig sac during postovulation (*Fig. 2C*).

The broad ligament near the paraovarian lymphatic plexus was thickened, and two layers of bulb-like lymphangions surrounded large blood vessels. Serial sections demonstrated that the size and position of the lymphangions varied with estrus. In the follicular phase, most of the lymphangions were separated from peritoneal mesothelium by a discontinuous muscle layer (*Fig. 3A*). When ovulating, lymphangions were in close contact with the mesothelium. Lymphatic lacunae in the submesothelium were numerous. Independent of the estrous cycle, these lymphatic lacunae were submesothelial and were seemingly in contact with the peritoneal cavity. Their endothelium and the mesothelium usually were in parallel; however, they were separated by a connective tissue layer (*Fig. 3B*). Characteristic foldings formed on the mesothelial surface (*Fig. 3C*) with submesothelial muscle cells. The upper portion of the mesothelial folds displayed cuboidal cells which became attenuated or disappeared in the "crypts." When lymphatic lacunae were visible, their endothelial cells were in direct contact with the folding mesothelium. Sac-like deep foldings were similarly depicted in cross-sections of the mesometrium but collector lymphatics exiting the plexus (*Fig. 2C*) were rarely observed. Close contact of collector lymphangions with the peritoneal surfaces was not well seen.

Silver staining demonstrated distinct types of mesothelial cells with anatomic localization by LM. Endothelial cell boundaries of both lymph and blood vessels were darkened similar to mesothelial cells. The first mesothelial cell type was approximately 18 µm in diameter had a flattened surface, and gently darkened

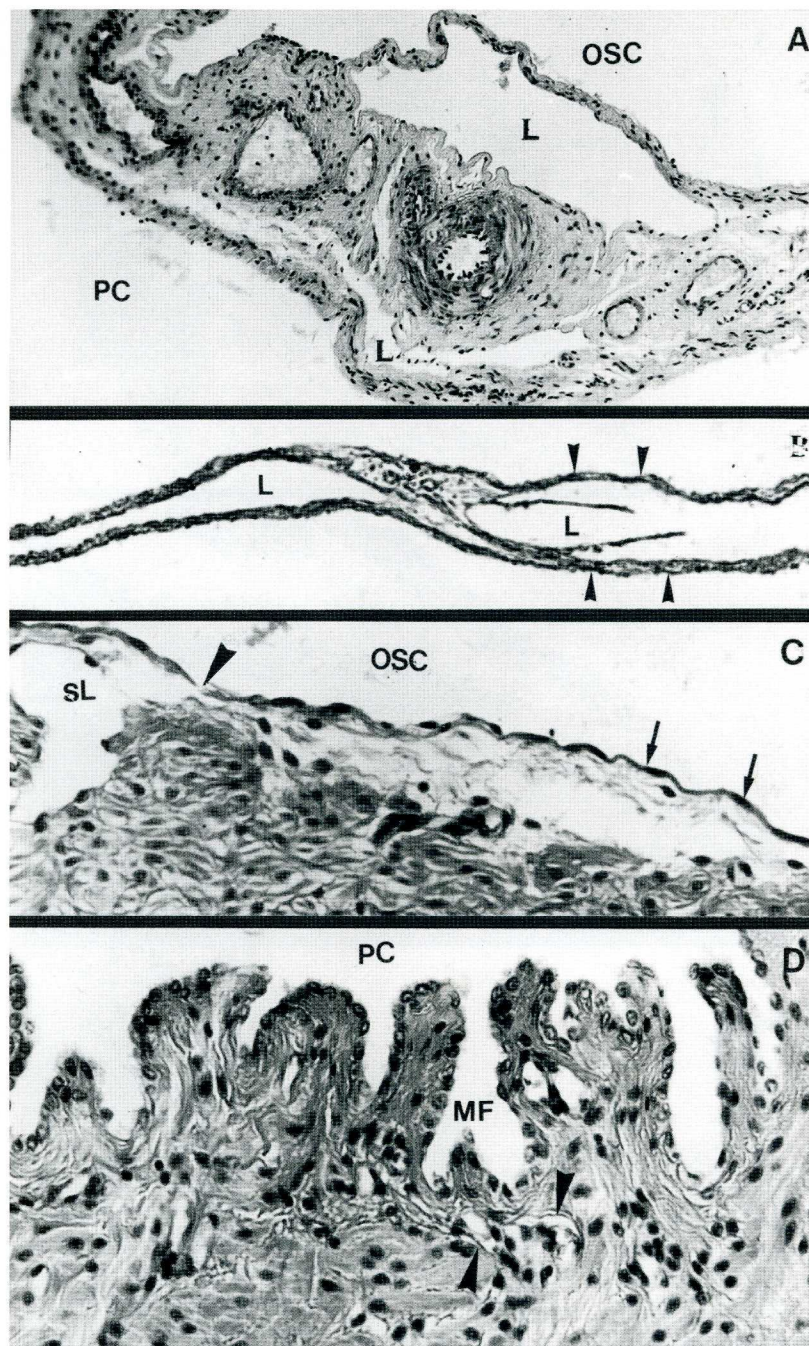


Fig. 2. Large lymphangions (L) near the margins of epithelial layers (A, x175) and compressed between two others (B, arrowheads; x125) and submesothelial lymphatic lacunae (sL) in direct contact with the paraovarian sac cavity (OSC) by a discontinuous epithelium (C, arrowhead; x500) in mesenteric wall of oviductal ampulla and infundibulum in early (A,C) and later (B) luteal phase. Mesothelial foldings (MF) and lymphatic capillaries (D, arrowheads; x500) in the superficial mesometrium which contains postplexus lymphatic collectors are also evident. OSC-paraovarian sac cavity, PC-peritoneal cavity, arrows (C)-endothelial cells rather than epithelial cells (compare with A). H&E.

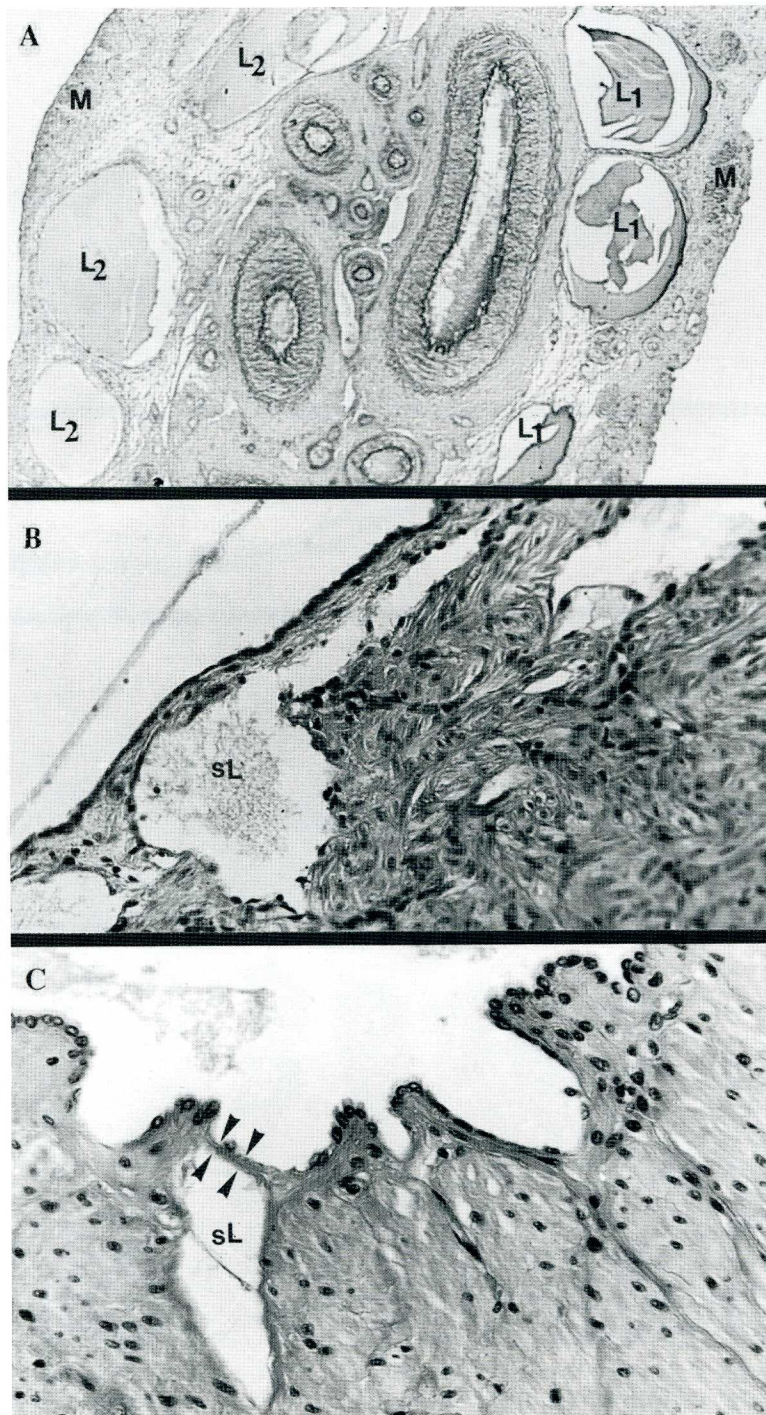


Fig. 3. The paraovarian lymphatic plexus. Large lymphangions filled with India ink (L1) and carmin-gelatin (L2) are seen beneath a discontinuous muscle layer (M) of the mesometrium in the luteal phase (A, x35). Lymphatic lacunae (sL) in the submesothelial connective tissue (B, x300) and between fascicles of muscle cells (C, x500). Note endothelium in contact with the mesothelium on the bottom of the mesothelial folding (arrowheads). H&E.

polygonal cell boundaries. The second cell type was smaller (8/12 μm), ovoid and with microprojections protruding into the peritoneal cavity with characteristic bands on the mesothelial layer (Fig. 4A). Stomatal depressions with silver deposits were also observed in various areas of smaller cells. Epithelial cell-free patches on the internal surfaces of the paraovarian sac were visible (Fig. 4B), especially postovulatory. By following lymph and blood vessels through superficial tissue layers (Figs. 4C-F), small mesothelial cells were depicted exclusively overlying lymphatic endothelial cells. The arrangement of epithelial cell-free segments was independent from the lymphatics (Fig. 4D). Endothelial cell contours and intercellular junctions of the lymphatics were conspicuous but opened interendothelial junctions were seldom visible during estrus. Most had closed preplexus lymphatic junctions in the follicular phase (Fig. 4E) and were open during the luteal phase in the area of the paraovarian lymphatic plexus (Figs. 4C and 4F).

Two variants of mesothelial cells and the connection with lymphatics in the paraovarian plexus were confirmed by SEM. At the peritoneal surface, the mesothelium was discontinuous and was characterized by indentations with exposed lymphatic endothelium and lymphatic stomata. A large portion of external and internal surfaces of the paraovarian sac under the infundibulum and ampulla were covered by cuboidal cells forming the lymphatic stomata. On external (Fig. 5A), stomatal orifices, the flattened perimeters of these cuboidal cells with continuous lymphatic endothelial cells formed various oval- or circular-sized rims (up to 20 μm in diameter), which varied during estrus. The internal lining of the paraovarian sac with epithelial cuboidal cells also varied during the estrous cycle, although lymphatic stomata with circular and irregular openings were uniformly prominent (Fig. 5B). Different cell types migrate through these openings (Figs. 5C and 5D), particularly after

ovulation. During the follicular phase, large regions of this lining surface exhibited lymphatic endothelial cells (Fig. 6A). Endothelial cells were elongated in shape and possessed smooth surfaces with occasional short microvilli (Fig. 6B). Crevice-like discontinuities between these cells and their contact with epithelial cells by their endings were also visualized. The surfaces of epithelial cells in these regions were characterized by innumerable microprojections extending from the lateral walls and forming a dense network over the endothelium. The superficial networks of epithelial-free channels with exposed connective tissue to the paraovarian sac cavum (Fig. 7A) were seen during the luteal phase, particularly right after ovulation. Such discontinuities of various sizes (to 20 μm in diameter) were spread beneath the oviduct, and the surface was covered with cuboidal and flattened cells. If the fibrous network was sparse, endothelial cells with different vasculature were seen (Fig. 7B). After the digestion of the tissues with 2N NaOH, thereby eliminating cellular elements and connective tissue matrix, the areas with intact collagen fibers displayed odd-looking sieve-like configurations with predominately thickened networks surrounded by dense bundles of collagen (Fig. 7C).

In areas with pre- and post-plexus lymphatic vasculatures, both mesothelial surfaces were almost completely composed of cuboidal cells (SEM). The regular and circular lines of cells on the visceral peritoneal layer of the uterus and oviduct isthmus (Fig. 8A) descended on the broad ligament and formed irregular discontinuous mesothelial cells (Fig. 8B). The stomata were numerous, the orifices had no surrounding rims, and were separated into several small compartments by bridges, lined with circular or irregular shaped pores, which opened onto underlying tissue. The circular and jagged openings in the stomatal orifices were visible primarily in the early luteal phase.

At the paraovarian plexus, both

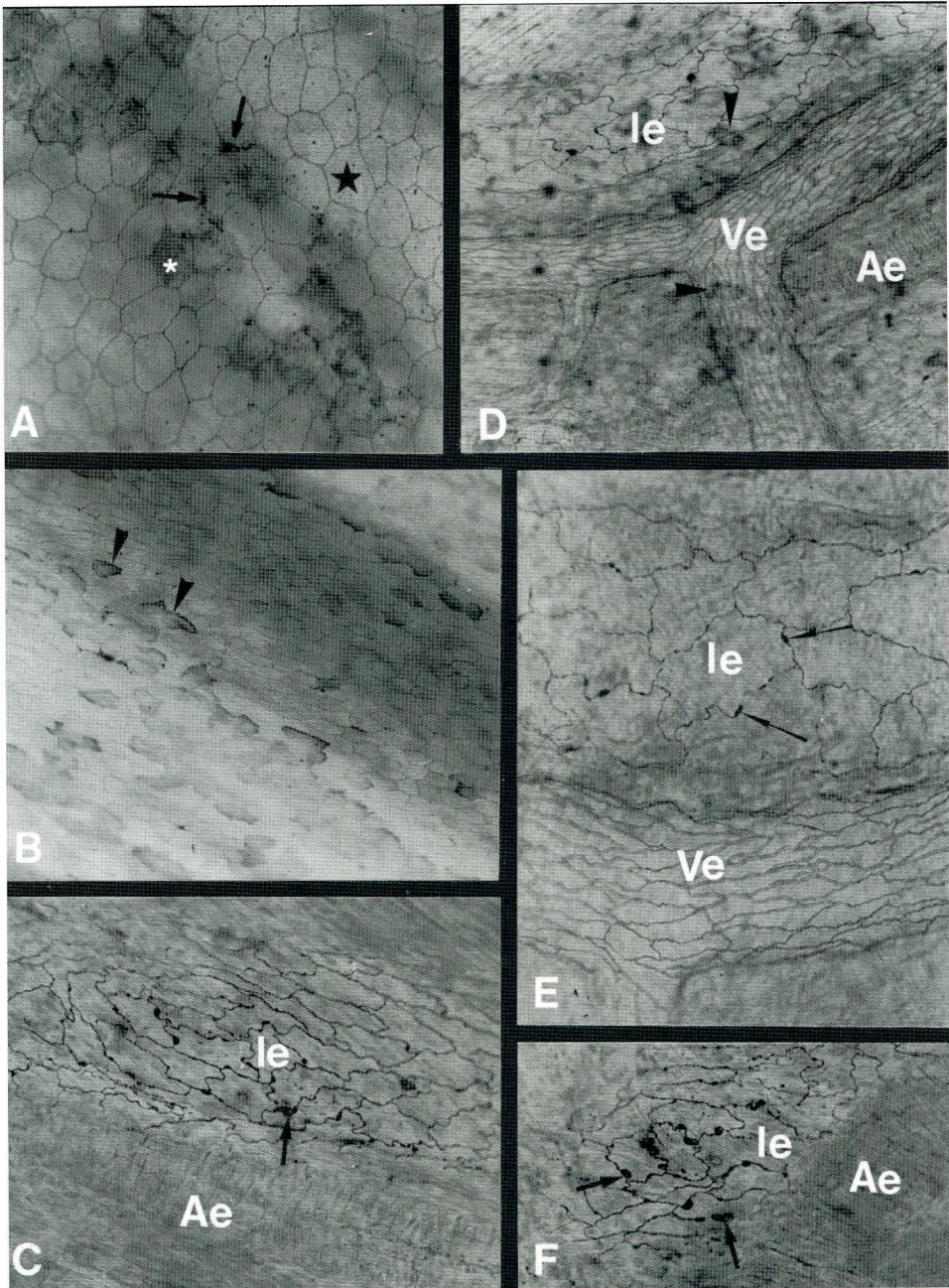


Fig. 4. Cell boundaries darkened with silver staining. In the mesothelial layer above the lymphatic plexus (A, x500) flattened polygonal cells (black asterisk) and bands of smaller cells with microprojections (white asterisk), and stomatal depressions with silver deposits (arrows) are visible. Epithelial cells (arrowheads) in the internal epithelium of the paraovarian sac in the luteal phase (B, x125) and located atop lymphatic (Le), venous (Ve), and arterial endothelium (Ae) as seen through the superficial tissue (D, x250). These cells are also seen within opened (thick arrows) and closed (thin arrows) interendothelial cell junctions in the region of the subovarian lymphatic plexus during the early (C, x250) and the late luteal phase (F, x250) and in preplexal lymphatics during the follicular phase (E, x500).

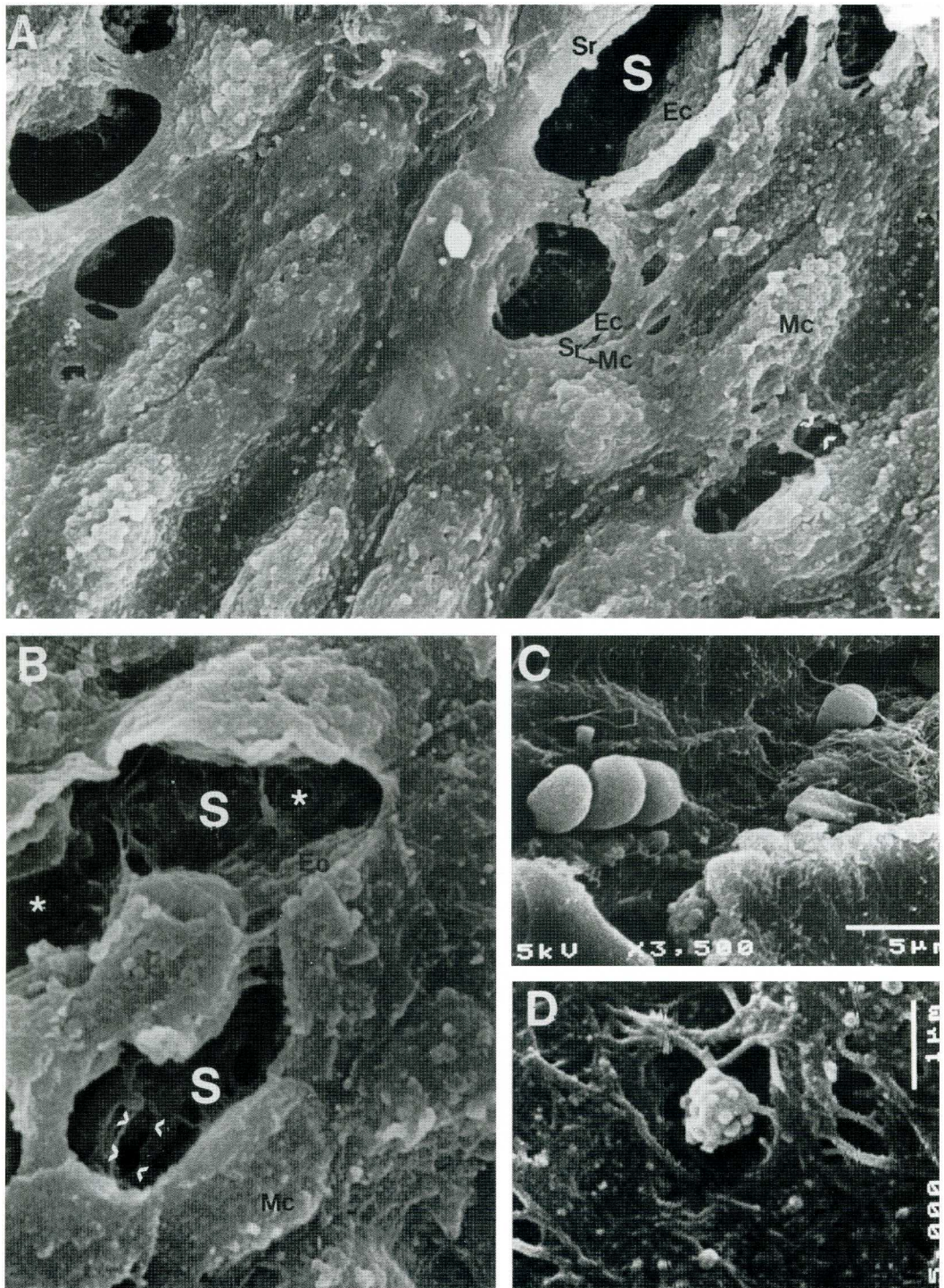


Fig. 5. SEM images of external (A, x3500) and internal (B, x3500) surfaces of the paraovarian sac with lymphatic stomata (S) and various cells migrating through the subendothelium (C,D). Sr—stomatal rims, asterisks—circular openings, arrowheads—irregular openings, Mc—mesothelial cells, Ec—endothelial cells.

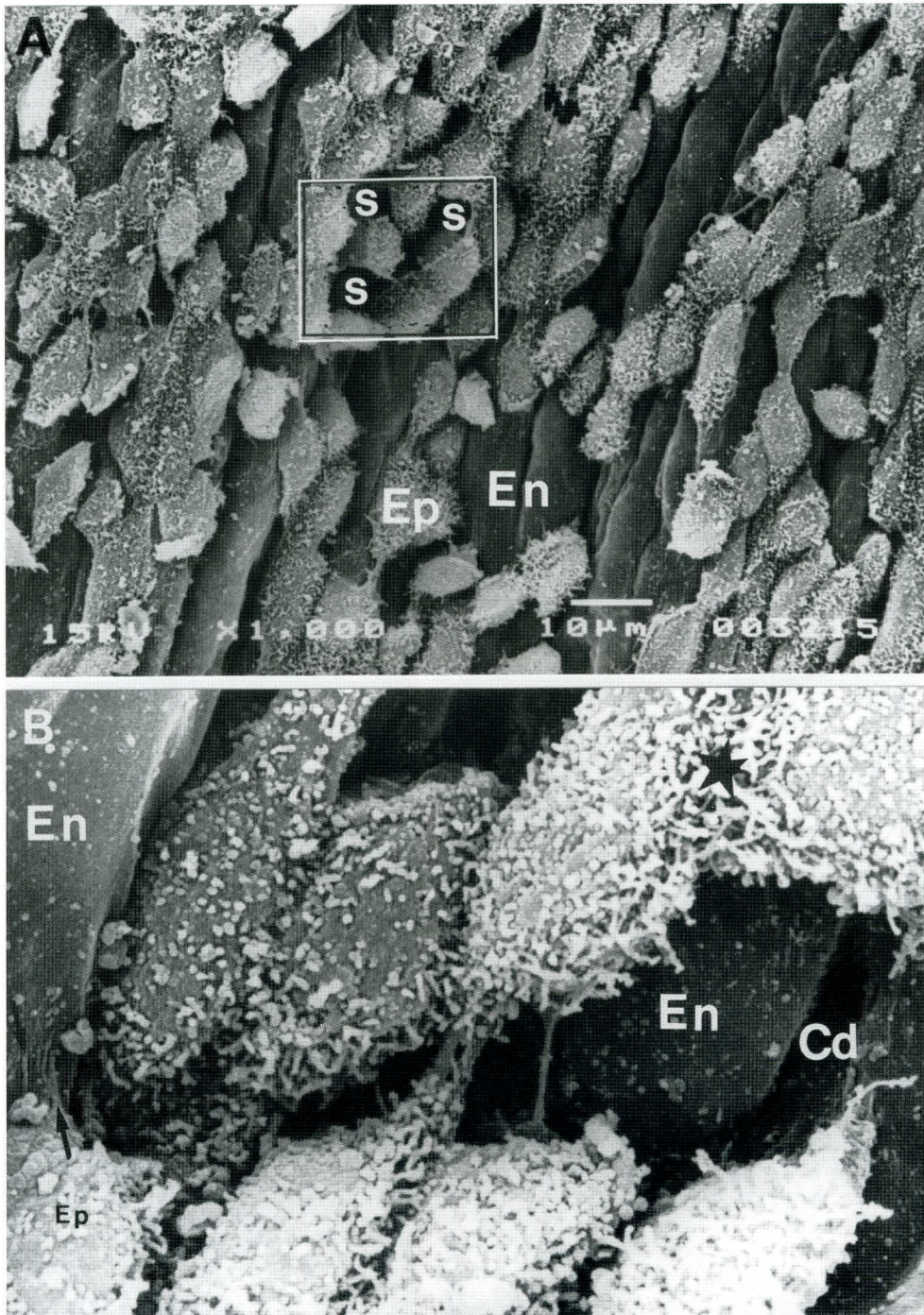


Fig. 6. SEM images of the internal lining of the paraovarian sac with epithelial (Ep) and lymphatic endothelial cells (En) during the follicular phase. The outlined fragment of Fig. 6A demonstrates three stomatal orifices (s), each formed by five epithelial cells. Magnified in Fig. 6B (x5000), the crevice-like discontinuities (Cd) between endothelial cells, the connection of endothelial and epithelial cells (arrows) and the network of epithelial microprojections above endothelial cells (asterisk) are well-depicted.

mesothelial layers displayed stomata with large oval orifices (average 50 μm in diameter) similar to those described on the external surface of the paraovarian sac. However, the stomatal openings were difficult to detect because the endothelial cell lining extended deeply. Circular openings (0.5-2.0 μm in diameter), however, in each phase of the estrous cycle were still visualized. In some stomata, large openings with jagged edges (to 10 μm in long diameter) also were visible (*Fig. 8C*), although mainly in the luteal phase. After digestion of the tissues with NaOH in comparable regions, collagen fascicles surrounding the loose network with single fibers were seen (*Fig. 8D*).

TEM disclosed that flattened cells lay on a continuous lamina densa, whereas cuboidal cells, similar to endothelial cells on submesothelial lymphatics, lay on a discontinuous lamina densa. Cuboidal cells were mostly observed directly atop the submesothelial lymphatics, whereas the more flattened cells covered the remaining surfaces which lacked submesothelial lymphatics. Although many ultra-thin sections from regions with lymphatics showed the mesothelial lining to be continuous, in other areas the peritoneal or the paraovarian sac cavities appeared continuous with the lymphatic lumen. Those continuous connections were evident when the margins of the surface cuboidal cells and underlying lymphatic endothelial cells were in direct contact with intercellular junctions. This close association was mainly between the processes of mesothelial cells and the thin ends of endothelial cells (*Fig. 9A*). The junctional contacts between these two different cell types were similar to macula or zonula adherentes. The intercellular connections were between cuboidal cells but tortuous intercellular clefts were also apparent from extensive overlapping and imbrications of adjacent marginal folds and pseudopoda-like processes. The widths of the intermesothelial clefts varied. Some connections of the lymphatic lacuna with the peritoneal cavity (as in the mesothelial layer

of the broad ligament in the utero-isthmal area) (*Fig. 9B*) were not detectable by SEM. The electron micrographs showed connections between the large paranuclear portions of the mesothelial cells and the free ends of the lymphatic endothelial cells, but the entry-communication was still restricted by plasma membranes forming a zonula adherens at the apex (*Fig. 9A*). Thus, the discontinuity of the communications emanated from the space between the extending processes of the mesothelial cells and not between lymphatic endothelial cells. Presumably, the pores or fenestrae as seen on the mesothelial surfaces by SEM were thereby preformed. Sections cut through the lymphatic stomata revealed that the circular openings as seen by SEM were defects formed between indentations of the lymphatic wall as depicted by TEM. The fenestration formed between the valve-like flaps of the endothelial cells using TEM corresponded to the jagged openings. Nonetheless, a definite link between the irregular openings of SEM and the fenestrae depicted by TEM was technically difficult to corroborate because of their minute size.

Typically, cuboidal cells and microvilli had thick cytoplasmic processes projecting from their free borders into the peritoneal or ovarian sac cavities. The nuclei of these cells were indented. The cytoplasm contained abundant, rough-surfaced endoplasmic reticulum (RER) in the form of long or short, irregularly-arranged cisterns, numerous free ribosomes and a well-developed Golgi apparatus, suggesting that these cells were functionally active (*Fig. 9A*). The round or elongated mitochondria were seen throughout the cytoplasm. Several cytoplasmic vesicles were also seen especially in the thinner margins of the cells. Coated vesicles and pits occurred along the cell borders, and some opened into the peritoneal or paraovarian sac cavities as well as the intercellular or subcellular spaces. The cytoplasm also contained microfilaments originating from and extending parallel to the base of the cuboidal cells. The flattened cells resembled

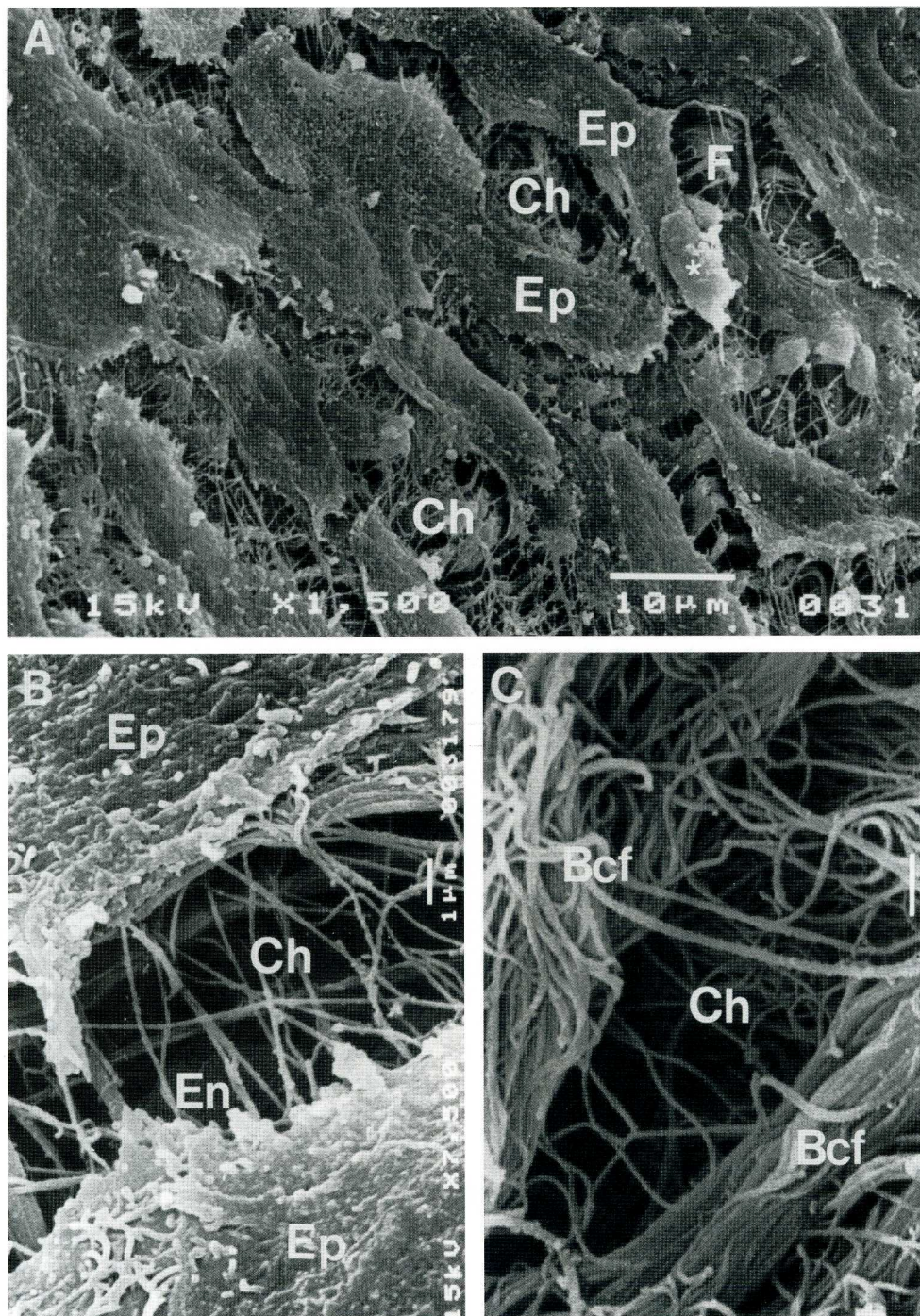


Fig. 7. SEM images of the superficial net of epithelial-free communications with connective tissue of the paraovarian sac cavity in early luteal phase (A). These connections are also seen both without (B) and with digestion of cellular elements (C). Ep—epithelial cells, Ch—interepithelial connections, F—fibroblast, asterisk—detached epithelial cell, Bcf—bundles of collagen surrounding the communication, En—endothelial cells beneath the connections.

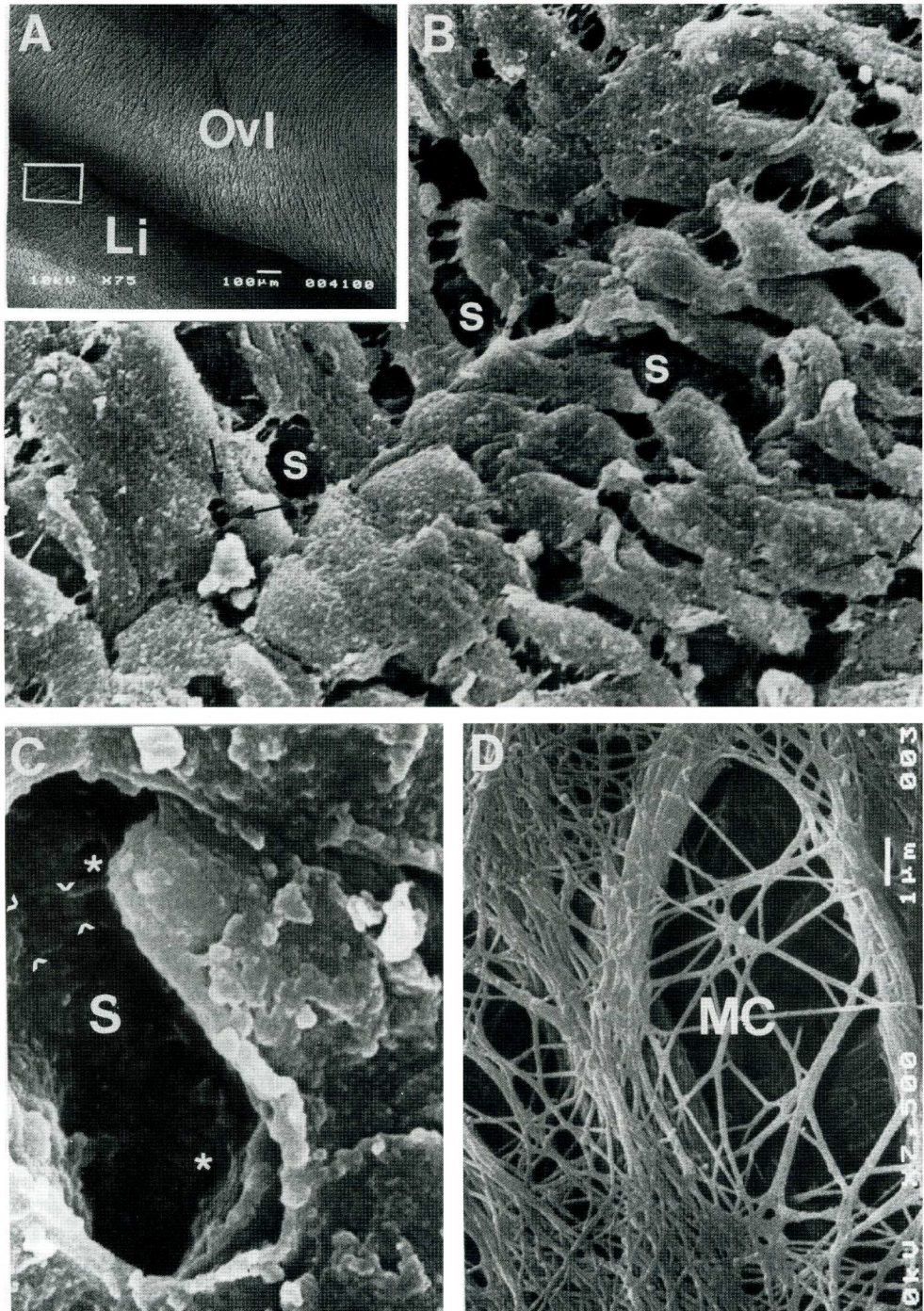


Fig. 8. SEM images showing a fragment of the oviductal-isthmus (Ovl) with broad ligament (Li) beneath the oviduct (A—insert) and several lymphatic stomata (s) and small pores (arrows) between layers of cuboidal cells (B, x1500). The stomata (s) with circular (asterisks) and irregular openings (arrowheads) (C, x5000) from the mesothelial layer of the paraovarian lymphatic plexus and sieve-like fibrous structure (Mc) after digestion by NaOH (D) are also seen.

cuboidal cells but they lined the continuous basal laminae, and thick cytoplasmic processes rarely extended from the cell border. The lymphatic endothelial cells of the submesothelial lacunae or lymphangions were usually thin and smooth at the borders with rare organelles. Their cellular cytoplasm characteristically contained fine filaments paralleling the longitudinal axis seemingly connecting the luminal and abluminal plasma membrane surfaces. Many vesicles and caveolae opened along the cell margins, mitochondria and RER profiles. Free ribosomes and polyribosomes were also seen in various compartments of the cytoplasm. The free ends or processes of endothelial cells in contact with mesothelial cells had few organelles (*Fig. 9A*). The cytoplasmic processes of endothelium occasionally extended into the adjacent connective tissue. The submesothelial connective tissue was "loose," particularly in areas with lymphatic lacunae. Between mesothelial and endothelial cells, anchoring filaments and an extracellular matrix on abluminal endothelial margins were visible. Collagen fibers were sparse when mesothelial and endothelial cells were adjacent but cross-sectional bundles of densely-packed collagen were near stomatal rims (*SEM*). These findings support that sieve-like fibrous structures (as observed after digestion with NaOH under *SEM*) represent a "scaffolding" for lymphatic stomata.

DISCUSSION

The complexity of lymphatic pathways that emanate from the pig uterus and reach the subovarian plexus (2) and the existence of three structurally and functionally different kinds of lymphangions during estrus (5) stimulated examination of lymphatics of the broad ligament and paraovarian sac.

The main morphological features delineated were connections between the pig lymphatic lumen and the peritoneal cavity and with the paraovarian sac cavity (18). Depending on the area, initial lymphatics

(capillaries) termed submesothelial lymphatic lacunae (19) and several large lymphangions (lymphatic segments) were in contact with mesothelial lining. The main preplexus pathway of the uterine lymphatics located in the subuterine-isthmus (2) and composed of lymphangions that regulate lymph flow during estrus (5) were interconnected by numerous lacunae. In the follicular phase, especially near ovulation, the lumen of the lymphangions was narrow, whereas in the luteal phase, the lumen had widened considerably. This cyclic change suggests a means of lymph transport between lacunae and the peritoneal cavity. These lymphatics are beneath the mesothelium, and the lymphatic endothelial cells often reach the base of the mesothelium; however, opened interendothelial junctions are not uniformly observed (*Fig. 4*). Closed interendothelial junctions were common in the follicular phase. In contrast, the lymphangions of pig oviductal lymphatics were located in the thin-walled paraovarian sac, connected with the epithelial cavity (see below). Nonetheless, in the thicker sac wall, lymphatic lacunae were evident. Similar observations were noticed in the closed capsule of the ovarian bursa in the golden hamster. Here, lymphatics were sandwiched between two layers of epithelium, abutting the peritoneal cavity and bursal cavities (14). The lymphangions of the subovarian plexus had very thin walls and resembled lymphatic capillaries. They were mainly composed of endothelium with a thickness akin to the size of a plasmalemma vesicle profile. In the luteal phase, the endothelium was freely suspended between lymph and subendothelial fluid. In the latter fluid, neighboring blood vessels were also suspended (5). Open endothelial junctions at this stage were common. The distance between the mesothelium and lymphatic lacunae varied but most often the endothelium and the discontinuous mesothelial layer were not separated by intervening tissue even in the submesothelial muscle. The relationship between the mesometrium and

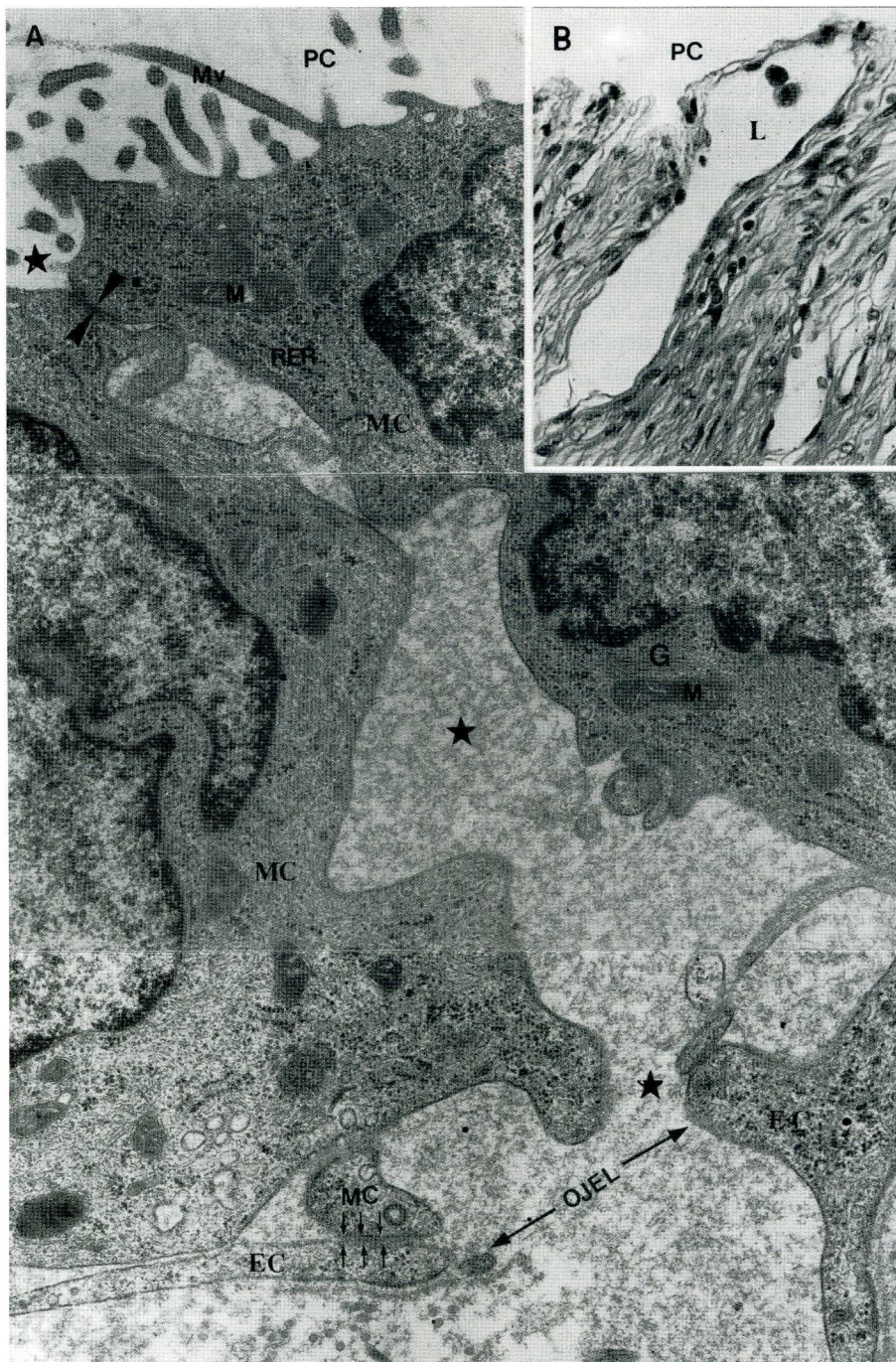


Fig. 9. TEM (A) and LM (B). A lymphatic lacuna with mesothelial cells lying directly beneath the mesothelium (B, x250). In A the connection (asterisks) is seen between paranuclear portions of mesothelial cells (MC) with free ends of the lymphatic endothelial cells (EC), although the entry site is limited by zonula adherens (arrowheads) at the apex (x 20000). PC—peritoneal cavity, N—nucleus, Mv—microvilli, G—Golgi apparatus, M—mitochondria, RER—rough-surfaced endoplasmic reticulum, OJEL—open junction between lymphatic endothelial cells, small arrows—zonula adherens between MC and EC.

lymphangions of the postplexus lymphatic collectors did not change with the estrous cycle (5), and displayed only small irregular contracted lymphatic capillaries which communicated with the mesothelium via the peritoneal cavity. Light microscopy (*Fig. 4*) showed that both surfaces of mesometrium and paraovarian sac were lined by a single layer of mesothelial (epithelial) cells that contained two different cell types. Smaller cuboidal cells, with stomata-like depressions darkened with silver deposits formed characteristic bands on the mesothelium above the lymphatic endothelium but not over arterial or venous endothelium. In 1903, Mac Callum (19) studying lymphatic lacunae in the submesothelial plexus of lymphatics depicted two morphologically-different profiles of mesothelial cells in the mouse diaphragm. In the non-lacunar areas, the cytoplasm appeared attenuated over major portion of the cell, whereas in the lacunae, the cells took on a cuboidal profile forming a dome-shaped contour projecting above the surface of the diaphragm. Cuboidal cells of the mesothelium overlying the lymphatic endothelium determined the "roof" of the lacunar spaces. Electron microscopy of the peritoneal surface of the diaphragm (20-23) has confirmed the non-uniform distribution of the mesothelium with two distinct cell populations according to whether they directly overlay the submesothelial lymphatic lacunae or cover the remaining areas of the diaphragm. Many areas of the superior mesothelium contained elements possessing stomata adjacent to the junction of cuboidal mesothelial cells. More than 130 years ago, Von Recklinghausen (24) described stomata as pores between mesothelial cells. Recent ultrastructural studies confirm these "stomata" which provide a direct link between the peritoneal cavity and lymphatics (13,20,21,25,27). Intraparietal injection of tracer particles have shown direct access to the lymphatic lacunar lumen (20,21,23,28).

The existence of stomata and associated connections is based upon specialized local

differentiation of the lacunar mesothelium, submesothelial connective tissue and lacunar endothelium, and the resultant formation of structurally distinctive units (20,21,23). Examples of direct communications between epithelial cells and endothelium are rare and are restricted to lymphatic drainage units of the peritoneal (20,21,23), pleural (29,30), pericardial (21), and ovarian bursa cavities (20,29-32). Shinohara et al (14) first described lymphatic stomata on the internal ovarian bursal wall of the golden hamster. These workers suggested that lymphatic stomata connect the bursal cavity with the lymphatic lumen and are present throughout the estrous cycle albeit somewhat dependent on changes in the ovarian bursal cavity. Direct communications demonstrated between epithelium and lymphatic endothelium, including larger lymphatics with valves both in the broad ligament and paraovarian sac walls in the pig verify characteristic features of reproductive serous membranes. In the pig, there are also consistent lymphatic stomata throughout estrus along precollectors of the subovarian lymphatic plexus. Stomatal orifices were formed by flattened cuboidal cells and represent the opposite of endothelial cell processes. These openings are connected by zonula or macula adherentes and are well depicted on the bordering rims of thin-walled endothelium and epithelium, which were either flattened or divided around the stomatal orifices or on the surface of the paraovarian sac (*Fig. 5A*). Circular and smooth surfaces lined by lymphatic endothelium and with opened stomata as described in the ovarian bursa of the golden hamster (15) were not found on the pig internal sac. Lymphatic endothelial cells, instead of sac epithelial cells, were detectable only near the ampulla and infundibulum during the follicular phase of estrus in the pig. Although there were crevice-like discontinuities between elongated endothelial cells, circular, oval, or other formed complexes of stomatal orifices remained where cuboidal cell lining existed. Epithelial

covering by lymphatic endothelium was not found in pigs in other phases of the estrous cycle. Endothelial cells in the internal layer of the paraovarian sac in the pig, albeit somewhat indefinite, has shown that smooth-surfaced areas lined with lymphatic endothelium on the inner surface of the hamster ovarian bursa appear during development in the prepubertal hamster 24 days postpartum (15). On the internal paraovarian sac surface of pigs in the luteal phase, however, it was surprising to find areas without cell covering. Because the subepithelial connective tissue is exposed to the sac cavity and is composed of various sized connections between collagenous fibers, we termed these structures, "the superficial networks of epithelial-free connections." They were dispersed throughout the surface with cuboidal and flattened cells and were mainly in the suboviduct ampulla and infundibulum. The circular defects or pores in the epithelial lining that exposed the subendothelial connective tissue were described in the ovarian bursa of the golden hamster (15). These pores were comprised mostly of the perimeters of cuboidal cells and appeared as though epithelial cells had become detached from the surface thereby opening the connective tissue to the bursal cavity. This connective tissue exposure to two different periovarian sacs, suggests damage to the internal epithelial layer during ovulation. NaOH degradation of cellular elements suggests in the epithelial layer of the pig ovarian sac, that there are dense-packed bundles of collagen which surround the superficial networks of epithelial-free connections. Perhaps loosely connected endothelial cells are easily detachable. Similarly, subpleural connective tissue is exposed to the pleural cavity through stomata (23,26,29,30). Shimada et al (11) using NaOH digestion and SEM to delineate the structure and function of the extravascular fluid pathway in monkey, rat, mouse, and rabbit diaphragm found that in the submesothelial connective tissue the maculae cribriformis is a

pre-lymphatic pathway. These "channels" were located between the mesothelium with stomata and initial lymphatics. In pigs, various lymphatic pathways of the paraovarian lymphatic plexus also suggest macula-cribriformis-like structures. However, in the area with cuboidal-cells consisting of lymphatic lacunae, only single collagen fibers formed a loose network albeit surrounded by densely-packed bundles of collagen.

Taken together, these morphological features suggest that fluid and particulate transport from the broad ligament and paraovarian region with adjacent peritoneal cavity is occurring via direct lymphatic luminal connections.

ACKNOWLEDGMENT

We thank Msc B Szerejko, Msc K. Jankowska and Ms D Zamaro for their excellent technical assistance with histological preparations. The study was carried out under grant no. 5 PD 6D 011 10 financed by the Committee for Scientific Research in Warsaw.

REFERENCES

1. Doboszynska, T, A Zezula-Szpyra: Morphological basis of the vascular paraovarian plexus functioning during the oestrous cycle in pig and sheep. II. SEM studies of corrosion casts of the arterial, venous and lymphatic vessels with special attention on side micro circulation network in the vasa-vasorum network of the paraovarian vascular plexus. *Rocz. Nauk Roln.*, SD 223 (1991), 38-96.
2. Gawronska, B, T Doboszynska, A Zezula-Szpyra: Light and scanning electron microscopy of the porcine mesometrial and paraovarian lymphatic networks. *Lymphology* 30 (1997), 26-35.
3. Gawronska, B, T Doboszynska, A Zezula-Szpyra: Lymphatic vessels in the broad ligament of the uterus in swine. *Lymphology* 25 (1992), 90-96.
4. Doboszynska, T, B Gawronska, A Zezula-Szpyra: The subovarian lymphatic plexus—an unknown structure within the broad ligament

- of the uterus in pig. Abstracts of the XIV Congress of the Polish Anatomical Society. Olsztyn, Poland (1993), 23-25.
5. Doboszynska, T, M Maksymowicz, A Andronowska, et al: The ultrastructure of lymphatic vessels emanating from the uterus and forming subovarian lymphatic plexus in pigs. *Folia Histochemica et Cytobiologica* 34 (suppl 1), (1996), 51-52.
 6. Doboszynska, T, A Andronowska, A Zezula-Szpyra, et al: Ultrastructural changes in mesometrial lymphatics during the oestrus cycle in pigs. *Folia Histochemica et Cytobiologica* 34 (suppl. 1), (1996), 53-54.
 7. Abu-Hijleh, MF, OA Habbal, ST Moqattash: The role of diaphragm in lymphatic absorption from the peritoneal cavity. *Review. J. Anat.* 186 (1995), 453-467.
 8. Kihara, T: Das extravasculare saftbahnsystem. *Okajimas Fol. Anat. Jpn.* 28 (1956), 601-621.
 9. Kihara, T: Studies on the system of extravascular fluid pathway. *Anat. Rec.* 26 (1960), 318.
 10. Shimada, T, F Sato, L Zhang, et al: Three-dimensional visualization of the aorta and elastic cartilage after removal of extracellular ground substance with a modified NaOH maceration method. *J. Electron Microsc.* 42 (1993), 328-333.
 11. Shimada, T, L Zhang, M Oya: Architecture and function of the extravascular fluid pathway: Special reference to the macula cribriformis in the diaphragm. *Acta Anat. Nippon* 70 (1995), 140-155.
 12. Clewe, TH: Absence of foramen in the ovarian bursa of the golden hamster. *Anat. Rec.* 151 (1965), 446.
 13. Shinohara, H, T Nakatani, T Matsuda: Postnatal development of the ovarian bursa of the golden hamster (*Mesocricetus auratus*): Its complete closure and morphogenesis of lymphatic stomata. *Am. J. Anat.* 179 (1987), 385-402.
 14. Shinohara, H, T Nakatani, T Matsuda: The presence of lymphatic stomata in the ovarian bursa of the golden hamster. *Anat. Rec.* 213 (1985), 44-52.
 15. Shinohara, H, T Nakatani, S Marisawa, et al: On the ovarian bursa of the golden hamster. I. Scanning electron microscopy of the inner surface and stomatal orifices. *J. Anat.* 147 (1986), 45-54.
 16. Rettberg, U: Licht- u. Elektronmikroskopische Untersuchungen über die Ureprünge u. Organism. Mesenterialer Lymphbahnen beim Meerschweinchen (*Cavia porcellus*). Kassel Univ. Diss. (1991), p. 1-141.
 17. Ohtani, O, T Ushiki, T Taguchi, et al: Collagen fibrillar network as skeletal frameworks. A demonstration by cell-maceration/scanning electron microscopic method. *Arch. Histol. Cytol.* 51 (1988), 249-261.
 18. Beck, LR: Comparative observations on the morphology of the mammalian periovarian sac. *J. Morphol.* 136 (1972), 247-254.
 19. Mac Callum, WG: On the mechanism of absorption of granular materials from the peritoneum. *Bulletin of Johns Hopkins Hospital* 14 (1903), 105-115.
 20. Tsilibary, EC, SL Wissing: Light and electron microscopic observation of the lymphatic drainage units of the peritoneal cavity of rodents. *Am. J. Anat.* 180 (1987), 195-207.
 21. Leak, LV, K Rahil: Permeability of the diaphragmatic mesothelium; the ultrastructural basis for "stomata". *Am. J. Anat.* 151 (1978), 557-592.
 22. Ji-Chang, L, Y Shou-Min: Study on the ultrastructure of the peritoneal stomata in human. *Acta Anat.* 141 (1991), 26-30.
 23. Abu-Hijleh, MF, RJ Scothorne: Regional lymph drainage routs from the diaphragm in the rat. *Clinical Anatomy* 7 (1994), 181-188.
 24. von Recklinghausen, F: Zur Fettresorption. *Arch. Pathol. Anat. Physiol.* 26 (1863), 172-208.
 25. Fukuo, Y, H Shinohara, H Matsuda: The distribution of lymphatic stomata in the diaphragm of the golden hamster. *J. Anat.* 169 (1990), 13-21.
 26. Negrini, D, M Del Fabbro, C Gonano, et al: Distribution of diaphragmatic lymphatic lacunae. *J. Appl. Physiol.* 72 (1992), 1166-1172.
 27. Nacatani, T, S Tanaka, S Mizukami, et al: Peritoneal lymphatic stomata of the diaphragm in the mouse. Process of their formation. *Anat. Rec.* 248 (1997), 121-128.
 28. Bettendorf, U: Lymph flow mechanism of the subperitoneal diaphragmatic lymphatics. *Lymphology* 11 (1978), 111-116.
 29. Wang, NS: The preformed stomas connecting the pleural cavity and the lymphatic in the parietal pleura. *Am. Rev. Resp. Dis.* 111 (1975), 12-20.
 30. Mariassy, AT, EB Wheeldon: The pleura: A combined light microscopic, scanning and transmission electron microscopic study in the sheep. I. Normal pleura. *Exp. Lung. Res.* 4 (1983), 193-313.
 31. Nacatani, T, H Shinohara, Y Fukuo, et al:

- Pericardium of rodents; pores connect the pericardial and pleural cavities. *Anat. Rec.* 220 (1988), 132-137.
32. Nacatani, T, H Shinohara, T Matsuda: On the ovarian bursa of the golden hamster. II. Intercellular connections in the bursal epithelium and passage of ferritin from the cavity into lymphatics. *J. Anat.* 148 (1968), 1-12.
33. Shinohara, H: Distribution of lymphatic stomata on the pleural surface of the thoracic cavity and the surface topography of the pleural mesothelium in the golden hamster. *Anat. Rec.* 249 (1997), 16-23.

Professor H. Teresa Doboszynska
Department of Reproductive
Histophysiology
Division of Reproductive Endocrinology &
Pathophysiology
Institute of Animal Reproduction and Food
Research of Polish Academy of Sciences
Prawochenskigo 5, P.O. Box 55
10-718 Olsztyn, POLAND
Telephone: /4889/5234658
Fax: /4889/5240347